Combining seroprevalence and capture-mark-recapture data to estimate the force of infection of brucellosis in a managed population of Alpine ibex

Sébastien Lambert, Emmanuelle Gilot-Fromont, Carole Toïgo, Pascal Marchand, Elodie Petit, Sophie Rossi, Anne Thébault

Title: Combining seroprevalence and capture-mark-recapture data to estimate the force of infection of brucellosis in a managed population of Alpine ibex

Author names and affiliations:

Sébastien Lambert [a*], Emmanuelle Gilot-Fromont [b], Carole Toïgo [c], Pascal Marchand [d], Elodie Petit [b,e], Sophie Rossi [f**], Anne Thébault [g]

[a] Université de Lyon, Université Lyon 1, CNRS, Laboratoire de Biométrie et Biologie Évolutive UMR 5558, Villeurbanne, France

[b] Université de Lyon, VetAgro Sup, CNRS, Laboratoire de Biométrie et Biologie Évolutive UMR 5558, Villeurbanne, France

[c] Office Français de la Biodiversité (OFB), Unité Ongulés Sauvages, Gières, France

[d] Office Français de la Biodiversité (OFB), Unité Ongulés Sauvages, Juvignac, France

[e] Office Français de la Biodiversité (OFB), Unité Sanitaire de la Faune, Sévrier, France

[f] Office Français de la Biodiversité (OFB), Unité Sanitaire de la Faune, Gap, France

[g] Agence nationale de sécurité sanitaire, de l'alimentation, de l'environnement et du travail (Anses), Direction de l'Évaluation des Risques, Maisons-Alfort, France

[*] Present address: Centre for Emerging, Endemic and Exotic Diseases, Department of Pathobiology and Population Sciences, Royal Veterinary College, University of London, Herts, UK

[**] The authors wish to dedicate this work to the beloved memory of Dr Sophie Rossi, who sadly passed away during the preparation of this manuscript. She dedicated her career to further the understanding of wildlife diseases and improve wildlife health, and her passionate work will remain an inspiration to us all.

Corresponding author: Dr Sébastien Lambert, Department of Pathobiology and Population Sciences, Royal Veterinary College, University of London, Hertfordshire, AL9 7TA, United Kingdom, selambert@rvc.ac.uk

Abstract: In wildlife, epidemiological data are often collected using cross-sectional surveys and antibody tests, and seroprevalence is the most common measure used to monitor the transmission dynamics of infectious diseases. On the contrary, the force of infection, a measure of transmission intensity that can help understand epidemiological dynamics and monitor management interventions, remains rarely used. The force of infection can be derived from age-stratified cross-sectional serological data, or from longitudinal data (although less frequently available in wildlife populations). Here, we combined seroprevalence and capture-mark-recapture data to estimate the force of infection of brucellosis in an Alpine ibex (*Capra ibex*) population followed from 2012 to 2018. Because the seroprevalence of brucellosis was 38% in this population in 2012, managers conducted two culling operations in 2013 and 2015, as well as captures every year since 2012, where seronegative individuals were marked and released, and seropositive individuals were removed. We obtained two estimates of the force of infection and its changes across time, by fitting (*i*) a catalytic model to age-seroprevalence data obtained from unmarked animals (cross-sectional), and (*ii*) a survival model to event time data obtained from recaptures of marked animals (longitudinal). Using both types of data allowed us to make robust inference about the temporal dynamics of the force of infection: indeed, there was evidence for a decrease in the force of infection between mid-2014 and late 2015 in both datasets. The force of infection was estimated to be reduced from 0.115 $year^{-1}$ [0.074–0.160] to 0.016 $year^{-1}$ [0.001–0.057]. These results confirm that transmission intensity decreased during the study period, probably due to management interventions and natural changes in infection dynamics. Estimating the force of infection could therefore be a valuable complement to classical seroprevalence analyses to monitor the dynamics of wildlife diseases, especially in the context of ongoing disease management interventions.

Keywords (5): wildlife disease management; force of infection; seroprevalence; catalytic model; survival analysis

INTRODUCTION

Recent outbreaks of wildlife diseases in Europe such as Chronic Wasting Disease or African Swine Fever have brought to light the need for effective, science-based disease management strategies in the wild (Mysterud and Rolandsen, 2018; Vicente et al., 2019). Depending on the host species and infectious disease considered, interventions such as culling, fencing, test-and-remove or vaccination have been implemented with various success in wild populations (le Roex et al., 2015; McDonald et al., 2008; Müller et al., 2015; Mysterud and Rolandsen, 2019). The first step in the choice of an appropriate management intervention is a sound evaluation of the epidemiological situation, in order to optimize strategies before any action is implemented (Artois et al., 2009). Then, ongoing management interventions should be accompanied by a close monitoring of both the infection and the population dynamics to assess their effectiveness (Joseph et al., 2013; Vicente et al., 2019). However, the management of wildlife diseases is often hampered by our limited knowledge of population and infection dynamics, and management actions are often implemented before a full picture of the situation has been drawn. It would therefore be desirable to extract the most information out of the available data to inform management decisions.

Incidence, i.e. the number of new infections in a population at risk over a given period of time, and prevalence, the proportion of infected individuals at a given point in time or over a certain period of time, are two common measures used to describe epidemiological dynamics of infections (Keiding, 1991). In wildlife populations, the collection of epidemiological data is often performed using cross-sectional surveys and serological (antibody) tests (Gilbert et al., 2013). Therefore, the prevalence of individuals positive to antibody tests (called seroprevalence) is often the only measure used to monitor the dynamics of infections in managed populations (Gilbert et al., 2013). However, the variation of seroprevalence over time provides only limited information on transmission dynamics, as the presence of

antibodies does not necessarily reflect active infections or inform on the timing of infection, especially in long-lived species. Unfortunately, incidence is rarely available for wildlife populations, because it requires longitudinal samplings of individual animals which are often logistically difficult (Gilbert et al., 2013). The force of infection (FOI), on the other hand, is a measure of transmission intensity related to incidence that can be obtained from age-seroprevalence data collected during cross-sectional surveys (Heisey et al., 2006) and that can help planning and optimizing management interventions (Lewis et al., 2014).

The FOI is the rate at which susceptible individuals become infected, and combines the contact rate, the probability of transmission given contact, and the number of infectious individuals in the population (Begon et al., 2002). Classical methods for estimating the FOI are based on the fact that the proportion of individuals who have ever been infected increases with age as a result of increased time of exposure to the infection (Heisey et al., 2006; Hens et al., 2010). These methods, also described as catalytic models (Muench, 1934), have been widely used for life-long immune infections in humans (Farrington, 1990; Keiding, 1991; Papoz et al., 1986). A common assumption in these models is that the FOI is constant over time, or at least constant on average (Hens et al., 2010), which is often not the case for diseases that are emerging or under management. Nonetheless, several studies were able to estimate time-varying FOI in humans (Katzelnick et al., 2018) and animals (Courtejoie et al., 2018). Estimating the FOI from age-seroprevalence data also has the additional advantage of assessing for infection-related mortality (Heisey et al., 2006; Reynolds et al., 2019).

The aim of this study was to estimate the FOI of brucellosis (*Brucella melitensis*) in Alpine ibex (*Capra ibex*) in the Bargy Massif (French Alps). This is the first reported example of self-sustained brucellosis infection in European wild-living ungulates, with a seroprevalence level as high as 38% at the beginning of monitoring in 2012-2013 (Garin-Bastuji et al., 2014; Hars et al., 2013). As France has been declared officially free of *Brucella melitensis* and

Brucella abortus in domestic ruminants since 2005 (Perrin et al., 2016a, 2016b), the persistence of *B. melitensis* in a wildlife population raises serious public health and economic concerns. This led the French authorities to undertake several management interventions since the discovery of the outbreak in 2012 (Lambert et al., 2018; Marchand et al., 2017). Among these, two massive culling operations were carried out in autumn 2013-spring 2014 (*n*=251 individuals culled, estimated population size before culling: 567, 95% CI [487-660]) and in autumn 2015 (*n*=70 individuals culled, estimated population size before culling: 344, 95% CI [290-421]). In parallel, the population was monitored by Capture-Mark-Recapture (CMR) to collect demographic and epidemiological data every year. During captures (*n*=387 between 2012 and 2018), a test-and-remove program was implemented where seropositive individuals were removed (*n*=119), while seronegative individuals were marked and released. The 2015 test-and-remove campaign was particularly intense with 38 individuals removed among the 125 captured.

As a consequence, cross-sectional data are available from unmarked animals, whereas the follow up of marked animals can be seen as data of a cohort study of seronegative animals. Contrary to the seroprevalence (Calenge et al., 2021; Marchand et al., 2017), the FOI has never been studied in the population before, although Calenge et al., 2021 estimated the FOI exerted on susceptible marked animals only, and assuming that it was proportional to the proportion of the total ibex population being seropositive, unmarked and actively infected. Therefore, we were interested in estimating the FOI from the available datasets to get a complementary picture of the epidemiological dynamics in the study population.

In ruminants, brucellosis is considered to produce lifelong infections, in particular in goats (European Commission, 2001; Schlafer and Miller, 2007), a species closely related to ibex. *Brucella* infection induces both humoral and cellular immune responses (Carvalho Neta et al., 2010; European Commission, 2001), which remains detectable over long periods of time

(Godfroid et al., 2010). The characteristics of brucellosis are therefore compatible with the use of catalytic models.

The presence of antibodies detected by serologic tests is used to detect previous exposure to *Brucella* (Godfroid et al., 2010). However, a potential issue with using antibodies as a proxy of past exposure is that infected individuals could be missed if antibody levels wane over time and decrease below detectable levels (Benavides et al., 2017). In elk (*Cervus canadensis*) infected with *B. abortus*, evidence suggest lifelong protective immunity but a progressive antibody loss after some years, which explains the decline in seroprevalence in older individuals (Benavides et al., 2017). In bison (*Bison bison*), a similar decline in seroprevalence in older individuals is observed (Treanor et al., 2011). This could be explained by the finding that active infections, which can be reactivated on favourable occasions such as oestrus or pregnancy (European Commission, 2001; Schlafer and Miller, 2007) and are associated with increased antibody levels (Durán-Ferrer et al., 2004), decreases with age in seropositive bison (Treanor et al., 2011).

In ibex, similar patterns have been found with a decline of seroprevalence in older individuals (Marchand et al., 2017) and a decrease of the probability of active infection with age (Lambert et al., 2018). Therefore, a partial antibody loss cannot be excluded; however, in the absence of relevant data to estimate this process, we assumed life-long infection and seropositivity in our study.

Infection-related mortality is another mechanism that could explain a decrease of seroprevalence with age (Benavides et al., 2017; Heisey et al., 2006). Therefore, one aim of the present study was to look for evidence of infection-related mortality, which can be estimated at the same time as the FOI (Heisey et al., 2006; Reynolds et al., 2019). Although there is currently no evidence for brucellosis-related mortality in the Alpine ibex population of the Bargy massif, it remains a possibility, e.g. because of brucellosis-related lesions such

157 as arthritis (Freycon et al., 2017). In other wild species, evidence for brucellosis-related
158 mortality were found in moose (*Alces alces*) and African buffalo (*Syncerus caffer*) (Forbes et
159 al., 1996; Gorsich et al., 2015), but not in bison or elk (Benavides et al., 2017; Fuller et al.,
160 2007; Joly and Messier, 2005).
161 Our study also aimed at evaluating temporal changes in the FOI between October 2012 and
162 June 2018. The seroprevalence did not change between 2012 and 2015 (Marchand et al.,
163 2017), when management interventions were dominated by massive culling operations.
164 However, a recent study demonstrated that it then decreased between 2015 and 2016, before
165 getting roughly stable from 2016 to 2018 (Calenge et al., 2021). Management interventions in
166 this second period were mainly based on test-and-remove during captures, especially in 2015
167 when 125 captures were achieved, followed by around 30-50 captures each following year.
168 Given this information, we hypothesized that the FOI also decreased between 2015 and 2016,
169 at the same time as the seroprevalence and following changes in the management
170 interventions. Alternatively, if individuals remain immune lifelong after infection, test-and-
171 remove of seropositive individuals could also increase the FOI by specifically removing
172 immune individuals (Ebinger et al., 2011). We also hypothesized that the FOI could change
173 in 2012, as there was no management in the study population before brucellosis was detected.
174 We therefore expected three periods, one before 2012, and two others between 2012 and
175 2018.
176

177 **MATERIAL AND METHODS**

178 **Population management and monitoring**

179 The study area, ibex population and discovery of *B. melitensis* infection have been described
180 previously (ANSES, 2015; Garin-Bastuji et al., 2014; Hars et al., 2013; Mailles et al., 2012;
181 Marchand et al., 2017; Mick et al., 2014).

182 The estimates of the population size were: 567 individuals (95% Confidence Interval: [487-
183 660]) in 2013, 310 [275-352] in 2014, 347 [290-421] in 2015, 272 [241-312] in 2016, 291
184 [262-327] in 2017 and 374 [326-435] in 2018 (Calenge et al., 2021; Marchand et al., 2017).
185 Between the beginning of the monitoring by CMR in October 2012 and summer 2018 (see
186 Figure 1 for the timing of captures and recaptures), a total of 387 captures and recaptures
187 have been performed (2012: 24, 2013: 57, 2014: 71, 2015: 125, 2016: 35, 2017: 27 and 2018:
188 48 – Lambert et al., 2020, 2018; Marchand et al., 2017). For each individual, information on
189 age (in years, by counting horn growth annuli, Michallet et al., 1988), sex, date of sampling
190 and spatial location of capture were systematically recorded. Captured animals were blood-
191 sampled by trained technical staff and serological tests were performed on serum samples.
192 The serological antibody tests were performed according to requirements of the European
193 Union for diagnosis of brucellosis in small ruminants and following standards of the World
194 Organization of Animal Health (OIE). Four serological tests were performed in parallel in
195 laboratory conditions: the Rose Bengal Test, the Complement Fixation Test, and the indirect
196 and the competitive Enzyme Linked ImmunoSorbent Assays. Individuals were considered as
197 seropositive when at least two of the tests were positive. Sensitivities and specificities of
198 these four tests for the diagnosis of *B. melitensis* in small domestic ruminants are generally
199 high: 75-100% and 97.6-100%, respectively (Blasco et al., 1994b, 1994a; Ferreira et al.,
200 2003; Nielsen et al., 2004). Although they remain unknown in ibex, the sensitivity and
201 specificity of the diagnosis protocol in ibex are considered high because of the use of
202 multiple tests in parallel and few cases of inconsistent results (ANSES, 2015). As part of a
203 test-and-remove program, captured individuals were either euthanized when they were
204 seropositive, or marked and released if they were seronegative at the time of sampling. Since
205 2015, the decision to euthanize ibex was based on the results of a rapid Lateral Flow
206 Immune-chromatographic Assay (LFIA), available for direct use in the field before

207 confirmation by the other tests in the laboratory. The LFIA had been validated on ibex samples
208 by the EU/OIE/FAO and National reference laboratory for animal brucellosis, showing very good
209 correlation with the four laboratory tests (ANSES, 2014; Corde et al., 2014).
210 In addition to CMR monitoring and test-and-remove operations, culling operations were also
211 implemented as part of the disease management strategy conducted by the French Authorities
212 (Figure 1). In spring 2013, four individuals showing clinical signs (e.g., lameness or presence
213 of visible gross lesions of the joints or the testes) were culled. In autumn 2013 and spring
214 2014, 233 and 18 individuals estimated to be older than 5 years were culled, based on the
215 observation that seroprevalence was significantly higher for this age class (Hars et al., 2013).
216 Non-selective culling of individuals that were never captured was also performed in autumn
217 2015 (n=70), autumn 2017 (n=5) and spring 2018 (n=5). The same antibody tests as in
218 captured animals were performed on culled ones whenever blood samples of good quality
219 were available. Among the 42 culled individuals for which results of serological tests were
220 available, the serological status of culled animals was based on a single LFIA test in a few
221 cases (n=12). This was also the case for one captured animal in 2015, and two marked
222 animals recaptured (all three with negative test results).
223
224 **Cross-sectional and longitudinal datasets**
225 In total, cross-sectional serological data were available from 363 unmarked individuals tested
226 between 2012 and 2018 (320 captured individuals, one found-dead individual and 42 culled
227 individuals– 129 seropositive and 234 seronegative results; Table S1). The first dataset we
228 used was therefore age-seroprevalence data from these unmarked individuals (Figure 2A,
229 Table S1 and Figure S1).
230 Among the seronegative individuals that were marked and released, 50 were recaptured at
231 least once during the study period and were tested again for antibodies against brucellosis.

The second dataset we used was therefore the follow up time (in days) between the first capture and the last recapture of marked animals. Because these animals were seronegative at the first capture, they either remained seronegative (n=46) or became seropositive in the interval (n=4 – Figure 2B and Figure S1). This type of data is also called "event time" data, where the event here would be the seroconversion from negative to positive. Individuals that seroconverted are "interval censored", i.e., the event of interest occurred between the last negative test and the positive test, but the exact time is not known (Kleinbaum and Klein, 2005). Conversely, individuals that remained seronegative at the last recapture are "right censored", i.e., the event of interest did not occur yet and may or may not occur in the future (Kleinbaum and Klein, 2005).

The longitudinal event time dataset covered the period 2012-2018, from first captures to last recaptures (Figure 2B), while the cross-sectional age-seroprevalence dataset covered the period from 1998 to 2018 (see below and Figure S1). The sample size for the longitudinal dataset (n=50) was also much smaller than for the cross-sectional dataset (n=363), because in the study population, most captures targeted unmarked individuals, in an attempt to test new individuals and maximise chances to remove infected individuals (Calenge et al., 2021). Indeed, marked ibex have more chances to be seronegative, as they already were during their last capture in a more or less recent past (Calenge et al., 2021).

Estimating the FOI using cross-sectional age-seroprevalence data

The FOI $\lambda(t)$ represents the rate at which susceptible individuals become infected per unit of time, at time t (Vynnycky and White, 2010), and can be calculated using the equation: $\lambda(t) = c\nu\frac{I(t)}{N(t)}$, where c is the contact rate, ν is the probability that the contact leads to infection, and $\frac{I(t)}{N(t)}$ is the proportion of infectious individuals in the population at time t (Begon et al., 2002).

The FOI changes over time, although its average value remains unchanged over time in endemic situations.

If we were to follow over time a cohort of individuals born the same year, we would observe that, as the cohort ages, the proportion of individuals who have ever been infected increases (in our case, the proportion of seropositive individuals as we are using seropositivity as a proxy of past infection). A cross-sectional sample would produce a similar pattern, as animals would be of different ages and therefore would have experienced various exposure times (Heisey et al., 2006). This has led to the development of the 'catalytic model' (Muench, 1934), that can be written as:

$$z(a) = 1 - e^{-\lambda a}$$

where $z(a)$ is the proportion ever infected at age a (in years), and λ is the average FOI (in years^{-1}). The main assumptions are that the average FOI λ is independent of age and year, that infection is lifelong or confers lifelong immunity, that all individuals are born without infection, and that susceptible and infected animals have the same mortality rate (i.e., no infection-related mortality experienced by infected animals).

When antibodies remain detectable lifelong, this model can be fitted to observed age-seroprevalence data to estimate the average FOI. However, the limitations related to the model assumptions led to new developments over the years, dealing for instance with age-dependent FOI (see Hens et al., 2010 for a review).

In this study, we used the general FOI model developed by Heisey et al. (2006) that allows for the existence of infection-related mortality in infected animals and the influence of covariates $X_1, \ldots, X_n$ on the FOI λ, leading to the new equation:

$$z(a) = \frac{1 - e^{-(\lambda-\mu)a}}{1 - \frac{\mu}{\lambda}e^{-(\lambda-\mu)a}}$$

where $z(a)$ is the proportion of seropositive at age a, μ is the infection-related mortality (infection being brucellosis in our case) and λ is the average FOI with $\lambda = \lambda_0 \, e^{\beta_1 X_1 + \cdots + \beta_n X_n}$, where λ_0 is the baseline FOI which is constant over age and time. Note that when $\mu = 0$, the equation simplifies to Muench's model: $z(a) = 1 - e^{-\lambda a}$. The model still assumes that all animals are born without infection, but can immediately leave this state and become positive (Heisey et al., 2006).

We tested for the existence of infection-related mortality by fitting this general FOI model to our age-seroprevalence data using a maximum likelihood approach and the R function currentstatus.1 provided in Heisey et al. (2006). We took into account the effects of sex and socio-spatial unit, which were demonstrated to play a major role in explaining variation in brucellosis seroprevalence in the study ibex population (Lambert et al., 2020; Marchand et al., 2017). Indeed, it has been highlighted that females transmit the infection in ~90% of cases (Lambert et al., 2020) and that they are spatially structured in five subpopulations with contrasted seroprevalence levels, the units at the centre of the massif ("core area") having the highest seroprevalence levels (Marchand et al., 2017).

We also tested the assumption that λ is independent of age. First, we added age (as a quantitative variable) among the covariates (Table 1), even though, in this case, the function for $z(a)$ would be incorrect, as it was obtained under the hypothesis that λ_0 was independent of age. However, this step is useful as a diagnostic tool, as if age or a function of age as covariate improves the model fit, it means that this assumption should be revised and functions other than constant with age should be explored for the baseline FOI (Heisey et al., 2006). Second, we used the piecewise constant hazards approach developed by Heisey et al. (2006) to enable the use of age-varying models for the baseline FOI λ_0 such as the Weibull, the Gompertz or the log-logistic models (Table S2).

Similarly, we added year of sampling (as a categorical variable) among the variables (Table 1), to test if the time-independence assumption holds (Heisey et al., 2006).

For each type of model (constant FOI, diagnostic model with covariate year – YEAR, diagnostic model with covariate age – AGE, diagnostic model with covariate quadratic age – AGE², diagnostic model with both AGE or AGE² and YEAR, Weibull, Log-logistic, Pareto, Gompertz), we fitted submodels including infection-related mortality (μ) or not, taking into account socio-spatial unit (UNIT) and sex (SEX) (Table 1 and Table S2). For each model, the number of parameters (degrees of freedom), the log-likelihood, the Akaike Information Criterion corrected for small sample sizes (AICc), and the difference between the AICc and the lowest AICc value (ΔAICc) were computed. The Akaike Weights, which are relative model likelihoods normalized over the likelihoods of all possible submodels, were computed using the function aictabCustom of the *AICcmodavg* R package (Mazerolle, 2019). The Akaike weight can be regarded as the conditional probability given the data of being the best model among the set of possible submodels (Wagenmakers and Farrell, 2004). We selected a set of models for which the ΔAICc was below two (Burnham et al., 2011; Burnham and Anderson, 2002).

Given that the selected models included the covariate year, we further explored the existence of temporal variation in the annual FOI by assuming a constant FOI with age but estimating different baseline FOI λ_0 for one, two or three periods of time to test our hypothesis. We therefore assumed that the FOI could be considered as time-independent on average for several years. This remains an approximation, but it allowed us to estimate temporal changes in the FOI while staying in the framework of the general FOI model.

Because births in ibex take place between the end of May and the beginning of July, we considered FOI of year *n* to start from July 1st year *n-1* up to July 1st year *n*. Based on age and years of sampling, individuals were born between 1998 and 2017. Because the monitoring

328 and management interventions started in 2012, the years 1998-2012 were always included in
329 the first period. We compared all possible models with two or three periods, using all
330 possible threshold years or couple of threshold years between 2012 and 2018 to obtain
331 different periods.
332 For each explanatory variable of the final model, results were expressed as Hazard Ratios
333 (HR). The hazard function is expressed as $\lambda = \lambda_0 e^{\beta_1 X_1 + \cdots + \beta_n X_n}$. For a single qualitative
334 covariate X that is either present ($X = 1$) or absent ($X = 0$), the hazard (FOI) is $\lambda = \lambda_0 e^{\beta}$ for
335 $X = 1$, and $\lambda = \lambda_0$ for $X = 0$. Therefore, the hazard ratio is $HR = \lambda_0 e^{\beta} / \lambda_0 = e^{\beta}$. Similarly,
336 hazard ratios can be expressed for qualitative covariates with multiple categories, and for an
337 increase in one unit of a quantitative covariate. Hazard ratios have a similar interpretation as
338 odds ratios (Dohoo et al., 2009). Profile likelihood 95% confidence interval around each
339 estimated coefficient were computed (Therneau and Grambsch, 2000).
340
341 **Estimating the FOI using longitudinal event time data**
342 As we were interested in the time until the occurrence of infection ("survival time"), we
343 analysed our longitudinal event time dataset using survival models. We note T the random
344 variable representing the time between the first capture and the infection event, in days. The
345 survival function is the probability that infection has not yet occurred by time t (follow up
346 time): $Surv(t) = P(T \geq t)$. Note that in our data, animals were captured for the first time at
347 different dates, meaning that the follow up time had different origins and therefore was not
348 equivalent to the calendar time (Figure S1).
349 The survival function can be related to the hazard function $\lambda(t)$, i.e., the rate at which the
350 event occurs per unit time, at time *t*, using the following equation (Kleinbaum and Klein,
351 2005):
352 $Surv(t) = e^{-\int_0^t \lambda(u)\, du}$

353 In our case, the event of interest is infection, and therefore the hazard function is the FOI.
354 Note that if we assume a constant hazard risk (FOI) with follow up time, the hazard function
355 is $\lambda(t) = \lambda$, and the corresponding survival function is $Surv(t) = e^{-\lambda t}$ (exponential model).
356 We tested the assumption that the hazard function is independent of age and calendar time,
357 using the exponential model from the function flexsurvreg of the *flexsurv* R package
358 (Jackson, 2016). We tested for the effects of age at last recapture (as a continuous variable,
359 calculated as the age at first capture incremented by the number of years between first capture
360 and last recapture) and year of recapture (as a categorical variable). Because of small sample
361 sizes, we had to group years 2014 and 2015 on the one hand and 2016 to 2018 on the other
362 hand. We were not able to take into account the effects of sex and socio-spatial unit because
363 of small sample sizes.
364 Given the results of the exponential model, we also explored the existence of variations with
365 calendar time, fitting models assuming two periods between 2012 and 2018 characterised by
366 two different FOI (independent of age and follow up time – Figure 2B). We fitted models
367 considering two periods, using all possible monthly threshold dates between November 2012
368 and June 2018, and compared them to the model considering a constant FOI.
369
370 **RESULTS**
371 **Force of infection estimated from cross-sectional age-seroprevalence data**
372 Among the twelve diagnostic models taking into account the effect of SEX and UNIT, all
373 models with ΔAICc<2 included the variable year, which suggests that the assumption of a
374 time-independent FOI is not appropriate (Table 1; see also parameter estimates in Table S3).
375 Models 9, 11 and 12 also included an age effect (Table 1). However, the effect sizes of linear
376 or quadratic age were small, and adding these effects to model 3 including the variable year
377 did not significantly improve model fit (Likelihood Ratio Tests: p=0.10 and p=0.09,

respectively). For completeness, we fitted several models of age-varying FOI using a piecewise constant hazards approach (models 13-20, Table S2). None of these models had a better AICc than model 3, which does not support variation of the FOI with age.

Two models (4 and 12) with ΔAICc<2 included infection-related mortality (Table 1). The effect sizes of the infection-related mortality in models 4 and 12 were small (Table S3), and adding infection-related mortality μ to model 3 or to model 11 did not significantly improve model fit (Likelihood Ratio Test: p=0.13 and p=0.52, respectively).

Given that all models with ΔAICc<2 included the variable year, we further explored the existence of temporal variation in the annual FOI by assuming a constant FOI with age and no infection-related mortality, but estimating different baseline FOI λ_0 for one (as a reference for no temporal variation), two or three periods of time.

The model with the lowest AICc (374.96; model 10 in Table S4) was obtained when considering three periods, with 2012 and 2015 as threshold years (Figure 3A and Table S4), and improved model fit compared to the model without temporal variation (AICc = 33.09, ΔAICc = 8.13 with model 10). Baseline FOI estimates and hazard ratios for the effects of SEX and UNIT are provided in Table S5: the FOI was highest in the second period, and lowest in the third period; it was higher for females than males, and for the socio-spatial units at the centre of the massif, where the seroprevalence levels are the highest. The average FOI over the whole population (from the same model with three periods but without effects of SEX and UNIT) was estimated to be 0.069 $year^{-1}$ [0.046–0.097] for the period 1998-2012, 0.115 $year^{-1}$ [0.074–0.160] for the period 2012-2015 and 0.016 $year^{-1}$ [0.001–0.057] for the period 2015-2018 (Figure 3B). A very similar model was obtained when considering three periods but with 2012 and 2014 as threshold years (Tables S4 and S5, Figure S2).

Force of infection estimated from longitudinal event time data

Using the exponential model (constant baseline hazard) to fit our event time data collected on marked animals, we found no significant effect of the variable AGE ($HR_{per\ year}$ = 0.81 [0.54-1.20], p=0.28), but a significant effect of the variable YEAR ($HR_{2014\text{-}2015\ vs\ 2016\text{-}2018}$ = 0.095 [0.009-0.92], p=0.043).

These results did not support variation of the FOI with age. However, given the significance of the variable YEAR, we further explored the existence of temporal variations in the FOI by fitting a model with two different periods on the calendar time, where individuals were submitted to different constant FOI before and after threshold dates. Among models considering all possible monthly threshold dates between November 2012 and June 2018, the best models (ΔAICc<2) were obtained when considering two periods with a threshold date between July 2014 and December 2015 (Figure 3C). The model with the lowest AICc was obtained when considering a threshold date in March 2015 (AICc = 30.72 – Figure 3C) and improved the model fit compared to the simple exponential model without temporal variations (AICc = 34.30, ΔAICc = 3.58). The FOI was estimated to be higher for the first period (0.086 $year^{-1}$ [0.015–0.193]) than for the second period (0 [0–0.030] – Figure 3D).

DISCUSSION

The aim of this study was to estimate the FOI of brucellosis in the wild Alpine ibex population of the Bargy massif (France) between 2012 and 2018. This measure of transmission intensity could help assess changes in transmission dynamics after management interventions started in 2012, as a complement to existing seroprevalence studies (Calenge et al., 2021; Marchand et al., 2017). Two massive culling operations were implemented in the population in 2013 and 2015. In addition, test-and-remove operations were performed during captures every year since 2012, with particularly high number of captures in 2015. We used two different datasets: age-seroprevalence data obtained from culling or first captures

428 operations (*n*=363), and event time data, derived from recaptures of marked animals (*n*=50).
429 In both datasets, the model selection process supported an effect of time on the FOI, and
430 returned estimates supporting a potential decrease of the FOI between mid-2014 and late
431 2015. The force of infection was estimated to be reduced from 0.115 $year^{-1}$ [0.074–0.160] to
432 0.016 $year^{-1}$ [0.001–0.057] in the age-seroprevalence data.
433 Longitudinal samplings are difficult to obtain in wild populations and are therefore often not
434 available (Gilbert et al., 2013). In our case, data from recaptured animals were available, but
435 the sample size remained relatively low (only four seropositive among 50 recaptured
436 animals), leading to large confidence intervals in the estimates of the FOI (e.g. [0.015–0.193]
437 $year^{-1}$ for 2012-2015). Although a higher number of recaptures may have provided a more
438 complete dataset, it would have had negative impact in terms of disease management. The
439 total number of captures each year being constrained for logistical reasons, focusing captures
440 on already marked animals would have led to less animals being captured for the first time,
441 and thus less seropositive animals being removed from the population. When management
442 actions and disease surveillance both rely on the same field actions, a compromise has to be
443 found between both objectives that may lead to gather less relevant surveillance data. In such
444 cases where longitudinal data are absent or scarce because of practical or management
445 reasons, the derivation of the FOI from cross-sectional serological data, more frequently
446 collected in wildlife, is a useful complementary approach to gain insights into the
447 epidemiological dynamics as we illustrated in our study.
448
449 **Model assumptions and infection-related mortality**
450 In both FOI models of cross-sectional and longitudinal data, the main assumption is the
451 independence of the FOI with age. We did not find any support for age-dependency in our
452 datasets (Table 1).

453 Estimating the FOI from age-prevalence data also had the advantage of bringing insights on
454 brucellosis-related mortality, for which we did not find strong evidence (Table 1). Our results
455 did not detect brucellosis-induced mortality in ibex, similar to studies in bison (Fuller et al.,
456 2007; Joly and Messier, 2005) or elk (Benavides et al., 2017).
457 We also postulated that the serological test has perfect sensitivity and specificity: due to the
458 use of multiple serological assays, previous studies estimated the sensitivity of diagnosis
459 protocol to be around 95%, with perfect specificity (expert assumption in ANSES, 2015;
460 Lambert et al., 2020). Test failure thus does not appear to be a high source of bias, however,
461 in the case of lower quality tests, other modelling approaches could be investigated (Bollaerts
462 et al., 2012; Buzdugan et al., 2017). A few individuals in our datasets only had results from
463 the rapid LFIA test used in the field (see Material and Methods). The analyses produced
464 qualitatively and quantitatively similar results when using reduced datasets without these
465 individuals (not shown).
466 In a former study, seroprevalence was found to decrease in old individuals, especially in
467 males (Marchand et al., 2017). It was hypothesized that this phenomenon could be explained
468 either by a lower survival rates or by lower probabilities to test positive in older individuals
469 infected by brucellosis (Marchand et al., 2017). We did not find strong evidence for
470 infection-related mortality, but we cannot exclude a decrease of antibody levels under
471 detectable levels as the animals age, which is difficult to reveal using seroprevalence data
472 (Heisey et al., 2006) (but see Benavides et al., 2017). Indeed, antibody titres measured by the
473 Complement Fixation Test appeared to decrease with age (Figure S3) (Lambert et al., 2018).
474 However, as high Complement Fixation Test titres are associated with active infections
475 (Durán-Ferrer et al., 2004), which are less often observed in old ibex (Lambert et al., 2018),
476 this may not reflect the antibody levels measured by the other serological tests used in the
477 study population. Unfortunately, the data for these other tests was not readily available.

Therefore, further studies investigating antibodies persistence with age or age-related variation in test performance is needed to firmly conclude about these results. Moreover, acquiring knowledge on antibody kinetics in ibex could have the additional advantage of developing alternative approaches that improve the derivation of the FOI by estimating the time since infection using individual data on antibody titres (Borremans et al., 2016; Pepin et al., 2017).

Finally, we also assumed, as classically done in catalytic models, that all individuals are born without infection. In domestic ruminants, congenital transmission of brucellosis exists but is rare, i.e., in only ca. 5% of kids born from infectious mothers (FAO and WHO, 1986; Godfroid et al., 2013). This transmission route is also suspected in ibex (Lambert et al., 2018), but is probably as uncommon as in domestic ruminants. Moreover, individuals congenitally infected seroconvert and become infectious only at the age of sexual maturity (Plommet et al., 1973). Therefore, we assumed that the effects would be negligible on our results.

Temporal variation of the force of infection

In Marchand et al. (2017), statistical analyses of seroprevalence data from 2012 to 2015 did not detect changes in seroprevalence before and after the mass culling of autumn 2013. Using a Bayesian approach to estimate seroprevalence, Calenge et al. (2021) found a strong decrease in the overall seroprevalence between 2015 and 2016. In the present study, both datasets suggest that the FOI decreased between mid-2014 and late 2015 (Figure 3), which could explain the seroprevalence drop also observed. Our results support a decrease in transmission during the study period, probably due to management interventions and natural changes in the infection dynamics. Quantitatively, seroprevalence was halved between 2015

and 2016 (Calenge et al., 2021), while FOI as estimated using age-seroprevalence data was divided by approximately ten at the same period (0.115 $year^{-1}$ *vs.* 0.016 $year^{-1}$).

In the process of estimating the seroprevalence in marked animals, Calenge et al. (2021) also estimated the FOI exerted on marked females in the core area, assuming it was proportional to the proportion of seropositive unmarked ibex with an active infection among the population of females in the core area. This analysis showed a decrease between 2015 and 2016, with estimates that were consistent with the values obtained with our longitudinal event time dataset where we did not make such assumptions on the relation between the FOI and active infections in the population (Calenge et al., 2021). Finally, an individual-based, stochastic SEIR mechanistic model, also showed a decrease in incidence between 2013 and 2016 in the whole population, and a low increase of new cases between 2016 and 2018. However, this increase in new cases was associated with a similar increase of population size which could indicate a constant incidence rate (Lambert et al., 2020). Therefore, the temporal dynamics appear to be consistent between the different approaches. The approach developed here has the advantage of being much simpler than the mechanistic model, and of bringing complementary information to previous seroprevalence analyses which can inform management decisions.

The FOI did not decrease between 2012 and mid-2014, even though the population size was halved due to massive culling operations in autumn 2013-spring 2014. On the contrary, our results showed that the FOI increased in 2012, which could be related to management interventions or undetermined natural changes in infection dynamics, such as abortion events that play a critical role in brucellosis transmission. We also demonstrated a decrease in the FOI in 2014 or 2015, which is probably related to management interventions. At the same time, test-and-remove during captures replaced massive culling as the main component of management strategies. However, our analyses cannot disentangle the effects of each

management intervention that were implemented between 2012 and 2015, and the intense test-and-remove operation of 2015 could have benefited from cumulative effects from the previous years. These hypothesis could be tested in the future using the stochastic SEIR mechanistic model developed in Lambert *et al.* (2020).

Unfortunately, we could not test for differences in temporal variation in the FOI between socio-spatial units (interactions between calendar time and spatial unit), due to low sample sizes. In a context where the FOI increases, such interactions could help to identify hotspots of infection, i.e., spatial units where the FOI increases faster, or simply different course of epidemics in the different spatial units (Heisey et al., 2010). Conversely, in a context of decreasing FOI such as in our study, interactions between calendar time and spatial units could reveal socio-spatial units with the sharpest decrease of FOI, which could correspond to areas where the management interventions are the most effective. In particular, management interventions since 2016 have been targeted towards the socio-spatial units at the centre of the massif, where the seroprevalence levels (and the FOI as demonstrated here) are the highest. It would therefore be interesting in the future to see if the FOI decreased faster in those units, and to test whether the FOI keeps decreasing in the units with less management interventions.

Force of infection in marked and unmarked animals

Our study aimed to compare the FOI between marked and unmarked animals. Most captures targeted unmarked individuals to maximise chances to remove seropositive individuals (Calenge et al., 2021). As a result, only a small number of marked animals were recaptured and a few cases of seroconversion were observed, leading to high uncertainty around the estimates of the FOI from the longitudinal event time dataset. Despite this uncertainty, the estimates from both datasets are comparable in each period (2012-2015 and 2015-2018) and

support a potential decrease of the FOI of similar magnitude. These results indicate that the FOI is similar in susceptible individuals from both groups, and therefore that marked individuals have similar patterns of exposure as unmarked individuals. Assuming similar FOI, a unified framework, using marked and unmarked animals, could be then further investigated to gain in precision of FOI estimates, even with relatively small longitudinal sample sizes, and better evaluate the requested sampling size of the monitoring (Gamble et al., 2020). An integrated framework combining cross sectional and longitudinal capture-recapture setups would also decrease the needed sample size in comparison with separate approaches (Gamble et al., 2020). It is worth noting that both our cross-sectional and longitudinal datasets are interval censored event time dataset: from birth to the positive test for the age-seroprevalence data or from negative to positive test for the longitudinal data. Therefore, future research could use both datasets in the same analyses, which will allow to increase the statistical power and to use more complex models of time-varying FOI.

CONCLUSIONS

In conclusion, using two distinct methods and datasets, our analyses revealed a decrease in the FOI between mid-2014 and late 2015, possibly as a result of the successive management operations implemented since 2012. Estimating the FOI can therefore provide valuable insights on the epidemiological dynamics, as a complement to classical seroprevalence analyses. This is especially the case in the context of ongoing disease management interventions in wildlife populations, where the FOI is expected to change. Insights on the effect of managing on transmission dynamics can be obtained using rather simple models as we did here, provided that there is no strong evidence that the basic assumptions are violated. Comparing two different sources of data, cross-sectional and cohort studies, with appropriate models may contribute to provide robust inference about the FOI. Nonetheless, it is possible

577 to derive FOI estimates from cross-sectional serological data only, which are the most
578 commonly available in wild populations.
579
580 **Acknowledgments**
581 The authors thank the two anonymous reviewers whose comments helped improve and
582 clarify this manuscript. The authors warmly thank all the field staff who performed
583 monitoring and management of the Alpine ibex population. They also thank the scientific
584 experts of the ANSES working groups on brucellosis of Alpine ibex in the Bargy massif, as
585 well as Charlotte Dunoyer (ANSES; UERSABA's chief unit) and Jean Hars (ONCFS). This
586 study was coordinated by the French Biodiversity Agency (Office Français de la Biodiversité,
587 OFB, formerly Hunting and Wildlife Agency, Office National de la Chasse et de la Faune
588 Sauvage, ONCFS). This work was performed within the framework of the LABEX
589 ECOFECT (ANR-11-LABX-0048) of Université de Lyon and of the program
590 "Investissements d'Avenir" (ANR- 11-IDEX-0007) operated by the French National
591 Research Agency (ANR).
592
593 **Funding**
594 This work was co-supported by the French Ministry of Research, the French Biodiversity
595 Agency (Office Français de la Biodiversité, OFB, formerly Hunting and Wildlife Agency,
596 Office National de la Chasse et de la Faune Sauvage, ONCFS), ANSES, and VetAgroSup
597 Lyon. The funders of the study had no role in the study design, the collection, analysis and
598 interpretation of data, the writing of the report, or the decision to submit the article for
599 publication.
600

Data availability statement: The raw data required to reproduce the above findings are available from the authors on reasonable request.

Declarations of interest: none

CRediT author statement

Sébastien Lambert: Conceptualisation, Methodology, Software, Formal Analysis, Data Curation, Writing – Original Draft, Writing – Review & Editing, Visualisation. **Emmanuelle Gilot-Fromont, Anne Thébault:** Conceptualisation, Methodology, Writing – Review & Editing, Supervision. **Carole Toïgo, Sophie Rossi:** Conceptualisation, Investigation, Writing – Review & Editing, Supervision. **Pascal Marchand, Elodie Petit:** Investigation, Data Curation, Writing – Review & Editing.

LITERATURE CITED

ANSES, 2015. Mesures de maîtrise de la brucellose chez les bouquetins du Bargy. Rapport ANSES.

ANSES, 2014. Note d'appui scientifique et technique de l'ANSES relatif au dépistage des bouquetins infectés de brucellose sur le terrain. Rapport ANSES.

Artois, M., Bengis, R., Delahay, R.J., Duchêne, M.-J., Duff, J.P., Ferroglio, E., Gortázar, C., Hutchings, M.R., Kock, R., Leighton, F.A., Mörner, T., Smith, G.C., 2009. Wildlife disease surveillance and monitoring, in: Management of Disease in Wild Mammals. pp. 187–214.

Begon, M., Bennett, M., Bowers, R.G., French, N.P., Hazel, S.M., Turner, J., 2002. A clarification of transmission terms in host-microparasite models: numbers, densities and areas. Epidemiol. Infect. 129, 147–153.

Benavides, J.A., Caillaud, D., Scurlock, B.M., Maichak, E.J., Edwards, W.H., Cross, P.C., 2017. Estimating loss of *Brucella abortus* antibodies from age-specific serological data in elk. EcoHealth 14, 234–243. https://doi.org/10.1007/s10393-017-1235-z

Blasco, J.M., Garin-Bastuji, B., Marin, C.M., Gerbier, G., Fanlo, J., Jimenez de Bagues, M.P., Cau, C., 1994a. Efficacy of different Rose Bengal and complement fixation antigens for the diagnosis of *Brucella melitensis* infection in sheep and goats. Vet. Rec. 134, 415–420. https://doi.org/10.1136/vr.134.16.415

Blasco, J.M., Marin, C.M., Jiménez-de-Bagués, M., Barberán, M., Hernández, A., Molina, L., Velasco, J., Diaz, R., Moriyon, I., 1994b. Evaluation of allergic and serological tests for diagnosing *Brucella melitensis* infection in sheep. J. Clin. Microbiol. 32, 1835–1840.

Bollaerts, K., Aerts, M., Shkedy, Z., Faes, C., Van der Stede, Y., Beutels, P., Hens, N., 2012. Estimating the population prevalence and force of infection directly from antibody titres. Stat. Modelling 12, 441–462. https://doi.org/10.1177/1471082X12457495

Borremans, B., Hens, N., Beutels, P., Leirs, H., Reijniers, J., 2016. Estimating time of infection using prior derological and individual information can greatly improve incidence estimation of human and wildlife infections. PLOS Comput. Biol. 12, e1004882. https://doi.org/10.1371/journal.pcbi.1004882

Burnham, K.P., Anderson, D.R., 2002. Model selection and multimodel inference: a practical information-theoretic approach, 2nd ed. ed. Springer, New York.

Burnham, K.P., Anderson, D.R., Huyvaert, K.P., 2011. AIC model selection and multimodel inference in behavioral ecology: some background, observations, and comparisons. Behav. Ecol. Sociobiol. 65, 23–35. https://doi.org/10.1007/s00265-010-1029-6

Buzdugan, S.N., Vergne, T., Grosbois, V., Delahay, R.J., Drewe, J.A., 2017. Inference of the infection status of individuals using longitudinal testing data from cryptic populations: towards a probabilistic approach to diagnosis. Sci. Rep. 7, 1–11. https://doi.org/10.1038/s41598-017-00806-4

Calenge, C., Lambert, S., Petit, E., Thébault, A., Gilot-Fromont, E., Toïgo, C., Rossi, S., 2021. Estimating disease prevalence and temporal dynamics using biased capture serological data in a wildlife reservoir: the example of brucellosis in Alpine ibex (*Capra ibex*). Prev. Vet. Med. 187, 1–12. https://doi.org/10.1016/j.prevetmed.2020.105239

Carvalho Neta, A.V., Mol, J.P.S., Xavier, M.N., Paixão, T.A., Lage, A.P., Santos, R.L., 2010. Pathogenesis of bovine brucellosis. Vet. J. 184, 146–155. https://doi.org/10.1016/j.tvjl.2009.04.010

Corde, Y., Drapeau, A., Game, Y., Maucci, E., Hars, J., Jaÿ, M., Garin-Bastuji, B., 2014. A rapid test for evaluating *B. melitensis* infection prevalence in an Alpine ibex (*Capra ibex*) reservoir in the French Alps. Presented at the Brucellosis 2014 International Research Conference, including the 67th Annual Brucellosis Research Meeting, Berlin, Germany, p. 221.

Courtejoie, N., Salje, H., Durand, B., Zanella, G., Cauchemez, S., 2018. Using serological studies to reconstruct the history of bluetongue epidemic in French cattle under successive vaccination campaigns. Epidemics 25, 54–60. https://doi.org/10.1016/j.epidem.2018.05.005

Dohoo, I., Martin, W., Stryhn, H., 2009. Veterinary epidemiologic research, 2. ed. ed. VER Inc, Charlottetown, Canada: University of Prince Edward Island.

Durán-Ferrer, M., Léon, L., Nielsen, K., Caporale, V., Mendoza, J., Osuna, A., Perales, A., Smith, P., De-Frutos, C., Gómez-Martín, B., Lucas, A., Chico, R., Delgado, O.D., Escabias, J.C., Arrogante, L., Díaz-Parra, R., Garrido, F., 2004. Antibody response and antigen-specific gamma-interferon profiles of vaccinated and unvaccinated pregnant sheep experimentally infected with *Brucella melitensis*. Vet. Microbiol. 100, 219–231. https://doi.org/10.1016/j.vetmic.2004.02.008

Ebinger, M., Cross, P., Wallen, R., White, P.J., Treanor, J., 2011. Simulating sterilization, vaccination, and test-and-remove as brucellosis control measures in bison. Ecol. Appl. 21, 2944–2959. https://doi.org/10.1890/10-2239.1

European Commission, 2001. Brucellosis in sheep and goats (*Brucella melitensis*) (No. SANCO.C.2/AH/R23/2001). Health & Consumer Protection Directorate-General, Brussels, Belgium.

Farrington, C.P., 1990. Modelling forces of infection for measles, mumps and rubella. Stat. Med. 9, 953–967. https://doi.org/10.1002/sim.4780090811

685 Ferreira, A.C., Cardoso, R., Travassos Dias, I., Mariano, I., Belo, A., Rolão Preto, I.,
686 Manteigas, A., Pina Fonseca, A., Corrêa De Sá, M.I., 2003. Evaluation of a modified
687 Rose Bengal test and an indirect Enzyme-Linked Immunosorbent Assay for the
688 diagnosis of *Brucella melitensis* infection in sheep. Vet. Res. 34, 297–305.
689 https://doi.org/10.1051/vetres:2003005
690 Forbes, L.B., Tessaro, S.V., Lees, W., 1996. Experimental studies on <i>Brucella abortus<i>
691 in moose (*Alces alces*). J. Wildl. Dis. 32, 94–104. https://doi.org/10.7589/0090-3558-
692 32.1.94
693 Freycon, P., Game, Y., Hars, J., Gilot-Fromont, E., 2017. Lesional aspects of *Brucella*
694 *melitensis* in *Capra ibex*. Bull. Acad. Vét. France 170, 1–5.
695 https://doi.org/10.4267/2042/62276
696 Fuller, J.A., Garrott, R.A., White, P.J., Aune, K.E., Roffe, T.J., Rhyan, J.C., 2007.
697 Reproduction and survival of Yellowstone bison. J. Wildl. Manage. 71, 2365–2372.
698 https://doi.org/10.2193/2006-201
699 Gamble, A., Garnier, R., Chambert, T., Gimenez, O., Boulinier, T., 2020. Next-generation
700 serology: integrating cross-sectional and capture–recapture approaches to infer
701 disease dynamics. Ecology 101, e02923. https://doi.org/10.1002/ecy.2923
702 Garin-Bastuji, B., Hars, J., Drapeau, A., Cherfa, M.-A., Game, Y., Le Horgne, J.M.,
703 Rautureau, S., Maucci, E., Pasquier, J.J., Jaÿ, M., Mick, V., 2014. Reemergence of
704 *Brucella melitensis* in wildlife, France. Emerg. Infect. Dis 20, 1570–1571.
705 https://doi.org/10.3201/eid2009.131517
706 Gilbert, A.T., Fooks, A.R., Hayman, D.T.S., Horton, D.L., Müller, T., Plowright, R., Peel,
707 A.J., Bowen, R., Wood, J.L.N., Mills, J., Cunningham, A.A., Rupprecht, C.E., 2013.
708 Deciphering serology to understand the ecology of infectious diseases in wildlife.
709 EcoHealth 10, 298–313. https://doi.org/10.1007/s10393-013-0856-0
710 Godfroid, J., Nielsen, K., Saegerman, C., 2010. Diagnosis of brucellosis in livestock and
711 wildlife. Croat. Med. J. 51, 296–305. https://doi.org/10.3325/cmj.2010.51.296
712 Gorsich, E.E., Ezenwa, V.O., Cross, P.C., Bengis, R.G., Jolles, A.E., 2015. Context-
713 dependent survival, fecundity and predicted population-level consequences of
714 brucellosis in African buffalo. J. Anim. Ecol. 84, 999–1009.
715 https://doi.org/10.1111/1365-2656.12356
716 Hars, J., Rautureau, S., Jaÿ, M., Game, Y., Gauthier, D., Herbaux, J.P., Le Horgne, J.M.,
717 Maucci, E., Pasquier, J.J., Vaniscotte, A., Mick, V., Garin-Bastuji, B., 2013. Un foyer
718 de brucellose chez les ongulés sauvages du massif du Bargy en Haute-Savoie. Bull.
719 Epidémiol. Santé Anim. Alim. 60, 2–7.
720 Heisey, D.M., Joly, D.O., Messier, F., 2006. The fitting of general force-of-infection models
721 to wildlife disease prevalence data. Ecology 87, 2356–2365.
722 https://doi.org/10.1890/0012-9658(2006)87[2356:TFOGFM]2.0.CO;2
723 Heisey, D.M., Osnas, E.E., Cross, P.C., Joly, D.O., Langenberg, J.A., Miller, M.W., 2010.
724 Linking process to pattern: estimating spatiotemporal dynamics of a wildlife epidemic
725 from cross-sectional data. Ecol. Monogr. 80, 221–240. https://doi.org/10.1890/09-
726 0052.1
727 Hens, N., Aerts, M., Faes, C., Shkedy, Z., Lejeune, O., Van Damme, P., Beutels, P., 2010.
728 Seventy-five years of estimating the force of infection from current status data.
729 Epidemiol. Infect. 138, 802–812. https://doi.org/10.1017/S0950268809990781
730 Jackson, R., 2016. Flexsurv: a platform for parametric survival modeling in R. J. Stat. Softw.
731 70, 1–33. https://doi.org/10.18637/jss.v070.i08
732 Joly, D.O., Messier, F., 2005. The effect of bovine tuberculosis and brucellosis on
733 reproduction and survival of wood bison in Wood Buffalo National Park. J. Anim.
734 Ecol. 74, 543–551. https://doi.org/10.1111/j.1365-2656.2005.00953.x

735 Joseph, M.B., Mihaljevic, J.R., Arellano, A.L., Kueneman, J.G., Preston, D.L., Cross, P.C.,
736 Johnson, P.T.J., 2013. Taming wildlife disease: bridging the gap between science and
737 management. J. Appl. Ecol. 50, 702–712. https://doi.org/10.1111/1365-2664.12084
738 Katzelnick, L.C., Ben-Shachar, R., Mercado, J.C., Rodriguez-Barraquer, I., Elizondo, D.,
739 Arguello, S., Nuñez, A., Ojeda, S., Sanchez, N., Mercado, B.L., Gresh, L., Burger-
740 Calderon, R., Kuan, G., Gordon, A., Balmaseda, A., Harris, E., 2018. Dynamics and
741 determinants of the force of infection of dengue virus from 1994 to 2015 in Managua,
742 Nicaragua. PNAS 115, 10762–10767. https://doi.org/10.1073/pnas.1809253115
743 Keiding, N., 1991. Age-specific incidence and prevalence: a statistical perspective. J. R. Stat.
744 Soc. Ser. A Stat. Soc. 154, 371–412. https://doi.org/10.2307/2983150
745 Kleinbaum, D.G., Klein, M., 2005. Survival analysis: a self-learning text, 2. ed. ed, Statistics
746 for biology and health. Springer, New York, NY.
747 Lambert, S., Gilot-Fromont, E., Freycon, P., Thébault, A., Game, Y., Toïgo, C., Petit, E.,
748 Barthe, M.-N., Reynaud, G., Jaÿ, M., Garin-Bastuji, B., Ponsart, C., Hars, J., Rossi,
749 S., 2018. High shedding potential and significant individual heterogeneity in
750 naturally-infected Alpine ibex (*Capra ibex*) with *Brucella melitensis*. Front.
751 Microbiol. 9, 1–15. https://doi.org/10.3389/fmicb.2018.01065
752 Lambert, S., Gilot-Fromont, E., Toïgo, C., Marchand, P., Petit, E., Garin-Bastuji, B.,
753 Gauthier, D., Gaillard, J.-M., Rossi, S., Thébault, A., 2020. An individual-based
754 model to assess the spatial and individual heterogeneity of *Brucella melitensis*
755 transmission in Alpine ibex. Ecol. Modell. 425, 109009.
756 https://doi.org/10.1016/j.ecolmodel.2020.109009
757 le Roex, N., Cooper, D., van Helden, P.D., Hoal, E.G., Jolles, A.E., 2015. Disease control in
758 wildlife: evaluating a test and cull programme for bovine tuberculosis in African
759 buffalo. Transbound. Emerg. Dis. [Epub ahead of print].
760 https://doi.org/10.1111/tbed.12329
761 Lewis, F.I., Otero-Abad, B., Hegglin, D., Deplazes, P., Torgerson, P.R., 2014. Dynamics of
762 the force of infection: insights from *Echinococcus multilocularis* infection in foxes.
763 PLoS Negl. Trop. Dis. 8, e2731. https://doi.org/10.1371/journal.pntd.0002731
764 Mailles, A., Rautureau, S., Le Horgne, J.M., Poignet-Leroux, B., d'Arnoux, C., Dennetière,
765 G., Faure, M., Lavigne, J.P., Bru, J.P., Garin-Bastuji, B., 2012. Re-emergence of
766 brucellosis in cattle in France and risk for human health. Euro Surveill. 17, 1–3.
767 Marchand, P., Freycon, P., Herbaux, J.P., Game, Y., Toïgo, C., Gilot-Fromont, E., Rossi, S.,
768 Hars, J., 2017. Sociospatial structure explains marked variation in brucellosis
769 seroprevalence in an Alpine ibex population. Sci. Rep. 7, 15592.
770 https://doi.org/10.1038/s41598-017-15803-w
771 Mazerolle, M.J., 2019. AICcmodavg: model selection and multimodel inference based on
772 (Q)AIC(c). R package version 2.2-2.
773 McDonald, R.A., Delahay, R.J., Carter, S.P., Smith, G.C., Cheeseman, C.L., 2008. Perturbing
774 implications of wildlife ecology for disease control. Trends Ecol. Evol. 23, 53–56.
775 https://doi.org/10.1016/j.tree.2007.10.011
776 Michallet, J., Grand, B., Bonardi, J., 1988. La population de bouquetins des Alpes du massif
777 de Belledonne-Sept Laux (département de l'Isère). Bull. Mens. ONC 19–24.
778 Mick, V., Le Carrou, G., Corde, Y., Game, Y., Jaÿ, M., Garin-Bastuji, B., 2014. *Brucella*
779 *melitensis* in France: persistence in wildlife and probable spillover from Alpine ibex
780 to domestic animals. PLoS ONE 9, e94168.
781 https://doi.org/10.1371/journal.pone.0094168
782 Muench, H., 1934. Derivation of rates from summation data by the catalytic curve. J. Am.
783 Stat. Assoc. 29, 25–38. https://doi.org/10.2307/2278457

Müller, T., Freuling, C.M., Wysocki, P., Roumiantzeff, M., Freney, J., Mettenleiter, T.C., Vos, A., 2015. Terrestrial rabies control in the European Union: historical achievements and challenges ahead. Vet. J. 203, 10–17. https://doi.org/10.1016/j.tvjl.2014.10.026

Mysterud, A., Rolandsen, C.M., 2019. Fencing for wildlife disease control. J. Appl. Ecol. 56, 519–525. https://doi.org/10.1111/1365-2664.13301

Mysterud, A., Rolandsen, C.M., 2018. A reindeer cull to prevent chronic wasting disease in Europe. Nat. Ecol. Evol. 1–3. https://doi.org/10.1038/s41559-018-0616-1

Nielsen, K., Gall, D., Smith, P., Balsevicius, S., Garrido, F., Durán-Ferrer, M., Biancifiori, F., Dajer, A., Luna, E., Samartino, L., Bermudez, R., Moreno, F., Renteria, T., Corral, A., 2004. Comparison of serological tests for the detection of ovine and caprine antibody to *Brucella melitensis*. Rev. Sci. Tech. Off. Int. Epizoot. 23, 979–987.

Papoz, L., Simondon, F., Saurin, W., Sarmini, H., 1986. A simple model relevant to toxoplasmosis applied to epidemiologic results in France. Am. J. Epidemiol. 123, 154–161. https://doi.org/10.1093/oxfordjournals.aje.a114210

Pepin, K.M., Kay, S.L., Golas, B.D., Shriner, S.S., Gilbert, A.T., Miller, R.S., Graham, A.L., Riley, S., Cross, P.C., Samuel, M.D., Hooten, M.B., Hoeting, J.A., Lloyd-Smith, J.O., Webb, C.T., Buhnerkempe, M.G., 2017. Inferring infection hazard in wildlife populations by linking data across individual and population scales. Ecol. Lett. 20, 275–292. https://doi.org/10.1111/ele.12732

Perrin, J.-B., Rautureau, S., Bronner, A., Hosteing, S., Dufour, B., Garin-Bastuji, B., Jaÿ, M., 2016a. Absence of bovine brucellosis confirmed in 2014, but vigilance must be maintained. Bull. Epidémiol. Santé Anim. Alim. 71, 12–16.

Perrin, J.-B., Rautureau, S., Bronner, A., Hosteing, S., Jaÿ, M., Garin-Bastuji, B., Dufour, B., 2016b. Brucellosis in small ruminants in 2014: 95 départements of metropolitan France are now officially disease-free. Bull. Epidémiol. Santé Anim. Alim. 71, 17–21.

Reynolds, J.J.H., Carver, S., Cunningham, M.W., Logan, K.A., Vickers, W., Crooks, K.R., VandeWoude, S., Craft, M.E., 2019. Feline immunodeficiency virus in puma: estimation of force of infection reveals insights into transmission. Ecol. Evol. 9, 11010–11024. https://doi.org/10.1002/ece3.5584

Schlafer, D.H., Miller, R.B., 2007. Female genital system, in: Maxie, M.G. (Ed.), Jubb, Kennedy & Palmer's Pathology of Domestic Animals (Fifth Edition). Elsevier, Edinburgh, pp. 429–431. https://doi.org/10.1016/B978-070202823-6.50174-3

Therneau, T.M., Grambsch, P.M., 2000. Modeling survival data: extending the Cox model, Statistics for biology and health. Springer, New York.

Treanor, J.J., Geremia, C., Crowley, P.H., Cox, J.J., White, P.J., Wallen, R.L., Blanton, D.W., 2011. Estimating probabilities of active brucellosis infection in Yellowstone bison through quantitative serology and tissue culture. J. Appl. Ecol. 48, 1324–1332. https://doi.org/10.1111/j.1365-2664.2011.02058.x

Vicente, J., Apollonio, M., Blanco-Aguiar, J.A., Borowik, T., Brivio, F., Casaer, J., Croft, S., Ericsson, G., Ferroglio, E., Gavier-Widen, D., Gortázar, C., Jansen, P.A., Keuling, O., Kowalczyk, R., Petrovic, K., Plhal, R., Podgórski, T., Sange, M., Scandura, M., Schmidt, K., Smith, G.C., Soriguer, R., Thulke, H.H., Zanet, S., Acevedo, P., 2019. Science-based wildlife disease response. Science 364, 943.2-944. https://doi.org/10.1126/science.aax4310

Vynnycky, E., White, R.G., 2010. An introduction to infectious disease modelling. Oxford University Press, New York.

Wagenmakers, E.J., Farrell, S., 2004. AIC model selection using Akaike weights. Psychon. Bull. Rev. 11, 192–196. https://doi.org/10.3758/BF03206482

Table 1: Model selection table to analyse the age-seroprevalence data using a constant force of infection with age and time, and testing for the effect of infection-related mortality μ, year and age (linear or quadratic), taking into account the effect of sex and socio-spatial unit.

N°	Year	Age	Age^2	μ	Unit	Sex	DF	LL	AICc	ΔAICc	W
11	**+**		**+**		**+**	**+**	**12**	**-176.91**	**378.73**	**0.00**	**0.20**
9	**+**	**+**			**+**	**+**	**12**	**-176.99**	**378.89**	**0.16**	**0.19**
4	**+**			**+**	**+**	**+**	**12**	**-177.16**	**379.24**	**0.50**	**0.16**
3	**+**				**+**	**+**	**11**	**-178.31**	**379.38**	**0.65**	**0.15**
12	**+**		**+**	**+**	**+**	**+**	**13**	**-176.71**	**380.48**	**1.75**	**0.09**
10	+	+		+	+	+	13	-176.99	381.04	2.31	0.06
7			+		+	+	7	-183.68	381.69	2.96	0.05
5		+			+	+	7	-184.20	382.73	3.99	0.03
2				+	+	+	7	-184.34	383.01	4.27	0.02
1					+	+	6	-185.42	383.09	4.35	0.02
8			+	+	+	+	8	-183.60	383.62	4.88	0.02
6		+		+	+	+	8	-184.20	384.82	6.09	0.01

For each model, the table gives the number of Degrees of Freedom (DF), the Log-Likelihood (LL), the Akaike Information Criterion corrected for small sample sizes (AICc), the difference between their AICc and the lowest AICc value (ΔAICc), and the Akaike Weights (W), which are relative model likelihoods normalized over the likelihoods of all possible submodels. The models with ΔAICc<2 are in bold.

Figure legends

Figure 1: Timing of the monitoring and management operations during which ibex of the Bargy massif (France) were sampled for serological tests between 2012 and 2018.
In green: months during which captures were performed; in yellow: months during which recaptures were performed; in blue: months during which culling operations were performed. The number of individuals captured, recaptured or culled is indicated for each operation.

Figure 2: Serological datasets for brucellosis between 2012 and 2018 in the Bargy massif (France)
(A) Age-seroprevalence data, for ibex culled or captured for the first time, with black points representing the observed seroprevalence for each age, with the size of the points proportional to the sample taken (n=363). (B) Distribution of the duration between the first capture (where the individuals were seronegative, marked and released) and the last recapture, where the ibex either tested seronegative, or converted to seropositive (the event of interest), for ibex that were recaptured at least once (n=50). (B) Dates of first capture and last recapture of marked individuals, for ibex that were recaptured at least once (n=50). The solid horizontal lines represent the life of marked animals between the date of their first capture, where they tested seronegative (white dots), and their last recapture, where they either tested seronegative or seropositive (black dots). The dashed vertical line represents a possible threshold date that separates the first period where individuals are exposed to a certain force of infection (FOI 1) from the second period where individuals are exposed to a different force of infection (FOI 2).

Figure 3: Estimates of time-varying forces of infection.
(A) AICc of the models considering different forces of infection for three periods on the calendar time for the cross-sectional age-seroprevalence dataset, comparing all possible pairs of threshold years between 2012 and 2017 to divide the 1998-2018 period into three. (C) AICc of the models considering different forces of infection for two periods on the calendar time for the longitudinal event time dataset, comparing all possible threshold months to divide the 2012-2018 period into two. In (A) and (C), the grey areas represents the AICc values where the difference between the AICc and the lowest AICc value (ΔAICc) were below two. (B) and (D) Estimates of the FOI ($year^{-1}$) for the best model considering time-varying forces of infection for the age-seroprevalence and the event time datasets, respectively, without effects of sex and unit. The lines represent the means, and the areas represent the 95% confidence intervals. The dashed vertical lines represent the threshold dates that separate the different periods corresponding to different forces of infection in the models with the lowest AICc values.

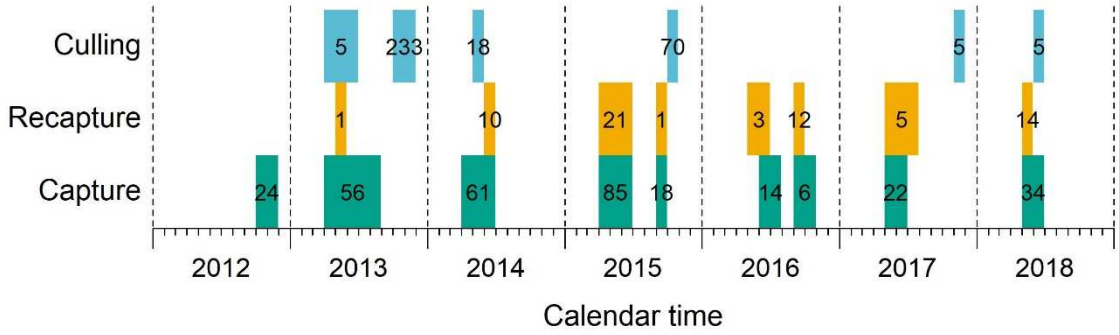

882
883 **Figure 1**

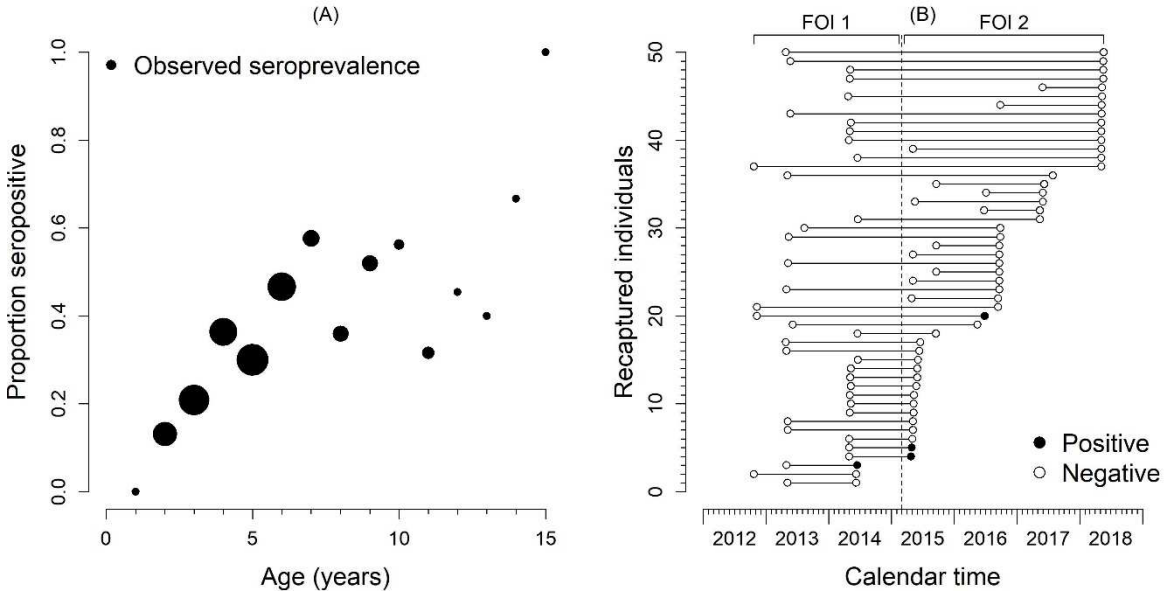

884
885 **Figure 2**
886

887

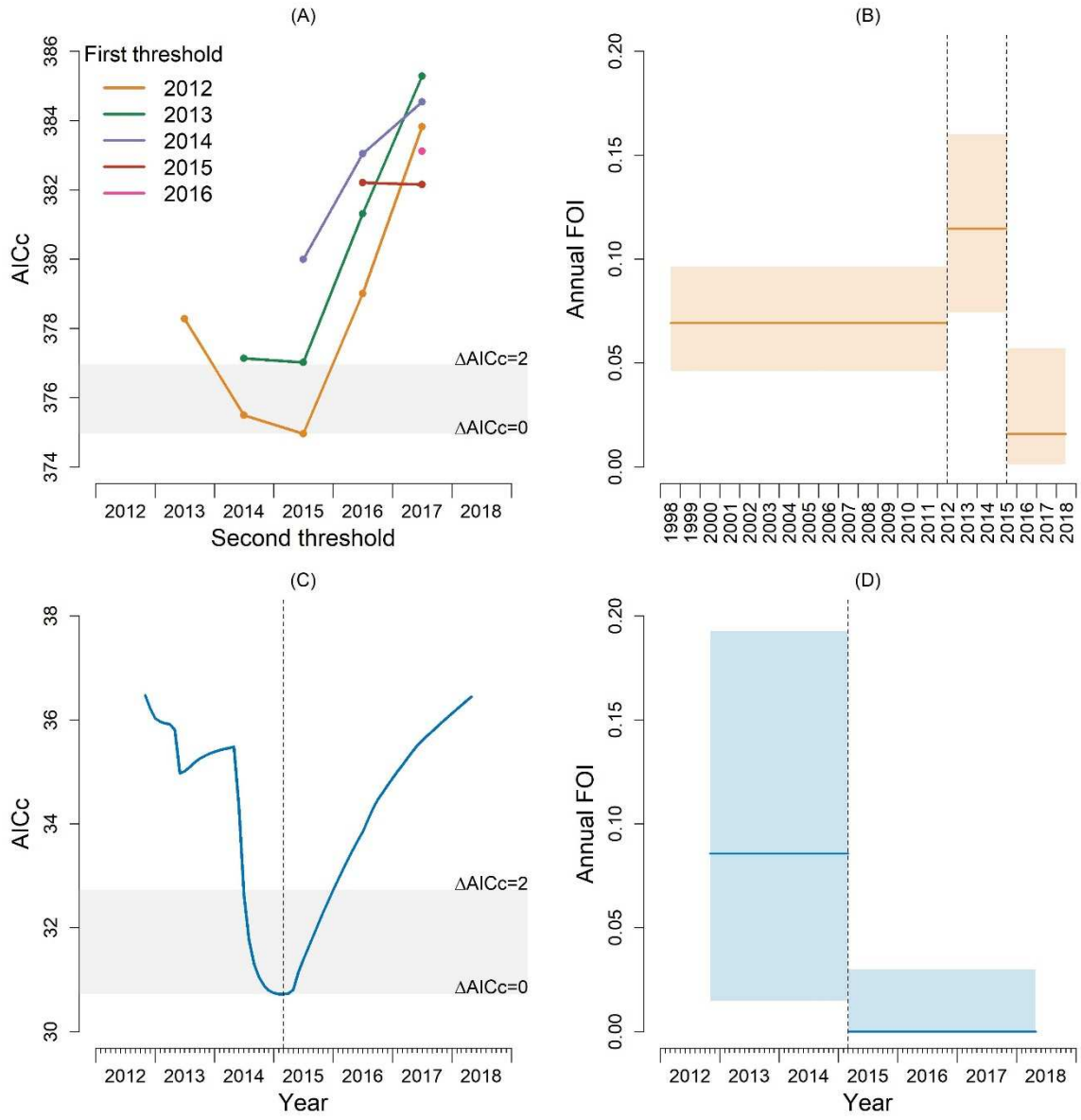

888
889 **Figure 3**